2nd International Conference on the Material Point Method for Modelling Soil-Water-Structure Interaction

Anura3D
MPM Research Community

Paper number: mpm2019.14
www.anura3d.com
www.mpm2019.eu

Modelling liquefaction using the Material Point Method – an evaluation using two constitutive models

Shreyas, Giridharan[1*], Dieter, Stolle[2], Christian, Moormann[1]
[1] Institute for Geotechnical Engineering, University of Stuttgart, Pfaffenwaldring 35, 70569 Stuttgart, Germany
[2] Department of Civil Engineering, McMaster University, 1280 Main Street West, Hamilton, Ontario, Canada

[*] E-mail: shreyas.giridharan@igs.uni-stuttgart.de

ABSTRACT

Different constitutive models have been developed that are capable of capturing the liquefaction effects in saturated soil subjected to dynamic loading. In this study, two well-known constitutive models for sandy soils have been chosen, the UBCSAND model and a hypoplastic sand (HPS) model. To numerically simulate the phenomena of seismic loading, the Convected Particle Domain Interpolation (CPDI) method, an advanced material point method (MPM), is employed. The numerical results from the UBCSAND model are compared against published experimental data. A comparison between the performance of UBCSAND and HPS model is presented by calibrating the former's properties to Berlin sand, which is already well documented for the HPS model. In this work, the shake table test performed at Rensselaer Polytechnic Institute is numerically simulated and is compared against the published experimental data.

KEY WORDS: MPM; CPDI; Liquefaction; UBCSAND; Hypoplastic Sand

INTRODUCTION

The phenomenon of liquefaction of saturated sands which causes significant damage to structures induced by seismic loading is quite frequent. Liquefaction takes place due to the accumulation of pore water pressure in loose saturated sandy soils under seismic loading. This phenomenon is usually accompanied by large amounts of ground subsidence, which serves as a trigger for damages of structures. Major earthquakes that occurred in times past such as the Niigata earthquake of 1964, Alaskan earthquake of 1964, Loma Prieta earthquake of 1989 or Hyogoken-Nambu earthquake of 1995 have demonstrated the destructive effects of soil liquefaction that accompanies a seismic event.

Seismic analyses based on finite element method allow an assessment of the liquefaction potential of a soil deposit, taking into account the pore pressure dissipation and the nature of loading. Such analyses are often time-consuming. Besides, the constitutive models require a large number of parameters to be calibrated to obtain a proper pore pressure generation. Alternatively, simplified methods are popular among practising engineers to assess the liquefaction risk in the preliminary design stages. If the liquefaction risk is high, a detailed finite element analysis can be carried out to obtain the pore pressure distribution and ground displacement. Simplified methods that are available for use are: (a) methods based on cyclic shear stresses generated in the soil, (b) probabilistic methods, and (c) energy-based methods. Despite the apparent drawbacks that the numerical methods pose to the user, finite element analysis of problems remains attractive due to its ability in capturing the physics behind the liquefaction. Combining a suitable constitutive model with the material point method, the large deformation that ensues liquefaction can be represented numerically, which has been restrictive in the classical finite element methods. The material point method together with the UBCSAND model, have been used to simulate seismic loading assuming saturated conditions in this work.

In order to accurately capture the complex dynamic behaviour of saturated soils assuming the numeric path, a robust finite element approach is required, along with a constitutive model that is capable of capturing the strength reduction in soil. Moreover, it bodes well if the finite element method, in addition to modelling the two-phase behaviour of soils accurately, is also able to capture the large deformations that accompany post-liquefaction. To

this end, a two-phase Convected Particle Domain Interpolation (CPDI), as an advancement to the classical Material Point Method (MPM) has been utilised (Sadeghirad et al., 2011). The two-phase formulation that contains particles consisting of both the soil and the water phase is utilised (van Esch et al., 2011). Two constitutive models are chosen for this study: (a) hypoplastic soil model with small-strain stiffness, which will be referred to as "HPS" model in this paper, and (b) UBCSAND model. The HPS model has been applied assuming saturated soil conditions for complex geotechnical applications with success (Moormann et al., 2018). HPS model's use has been prevalent in the geotechnical community, which is attributed to the model being quite versatile in its ability to model both static and cyclic loads, and it's availability as an add-on UMAT file for various commercial finite element packages. UBCSAND is a two-dimensional elasto-plastic model capable of capturing the liquefaction effects that occur in soil during seismic loading (Puebla et al., 1997). The model that is used in this study is the one reported in the work of Naesgaard (2011).

To test the implementation of the constitutive model into the two-phase CPDI code, a well-known case study of a shake table test is modelled (Byrne et al., 2004). The numerical results are compared with the published experimental data to examine the capability of the UBCSAND constitutive model, together with the CPDI code, to capture the measured results. The applicability of HPS model is also compared against the UBCSAND model for the benchmark case.

The paper is divided as follows. A brief overview of the numerical setup of the model is provided, followed by the setup and results of the shaking table test. A comparison between the HPS model and the UBCSAND model is drawn, followed by the conclusions.

NUMERICAL SETUP

An extensive literature survey on the finite element implementation of fully-saturated two-phase problems is presented in detail in the work of Zienkiewicz et al. (1990). Simplified governing equations were presented along with early results of seismic load induced liquefaction. Although it was shown that the *v-p* formulation, i.e., the solid-velocity water pressure formulation can indeed capture dynamic responses for varied scenarios, it has been shown that the formulation cannot adequately represent the two-phase dynamic behaviour (van Esch et al., 2011). An alternative approach utilizing a full set of equations for the soil and water phase is considered, the *v-w* formulation. The momentum equations for both the solid and water phases are given by,

$$\rho_w \frac{dv_{j,w}}{dt} = \frac{\partial p}{\partial x_i} + \rho_w g_j - \frac{n \rho_w g}{k}\left(v_{j,w} - v_{j,s}\right) \tag{1}$$

$$(1-n)\,\rho_s \frac{\partial v_{j,s}}{\partial t} = -n\,\rho_w \frac{\partial v_{j,w}}{\partial t} + \frac{\partial \sigma_{ij}}{\partial x_i} + \rho_{sat}\, g_j \tag{2}$$

where, ρ_w, ρ_s and ρ_{sat} are the water, solid and saturated soil densities, respectively. The subscripts i, j refer to the directions, g_j refers to the gravity in the x_j-direction, and $v_{j,w}$ and $v_{j,s}$ are the velocity of fluid and solid phases, respectively. σ_{ij} is the total stress tensor, k is the hydraulic conductivity of soil and n the porosity. Equation 1 contains the drag term, corresponding to Darcy's law. Pore pressure rate is calculated using the mass balance equation that serves as the constitutive law for the water, given by

$$\frac{dp}{dt} = \frac{K_w}{n}\left[(1-n)\frac{\partial v_{j,s}}{\partial x_j} + n\frac{\partial v_{j,w}}{\partial x_j}\right] \tag{3}$$

where K_w is the bulk modulus of the water phase. Total stress in the soil is then calculated using the relation

$$\sigma_{ij} = \sigma'_{ij} + p\delta_{ij} \tag{4}$$

with the effective stress being obtained from the constitutive model for the soil.

Effective stress numerical setup for UBCSAND model

Elastic response

The elastic response of the model is assumed to be isotropic, in which the shear modulus G^e, and the bulk modulus B^e are given by relations,

$$G^e = K_G^e \cdot Pa \cdot \left(\frac{\sigma'}{Pa}\right)^{n_e} \tag{5}$$

$$B^e = K_B^e \cdot Pa \cdot \left(\frac{\sigma'}{Pa}\right)^{m_e} \tag{6}$$

Here, Pa is the atmospheric pressure, chosen as 100 kPa for all simulations in this work, σ' is the mean effective stress, and n_e and m_e are elastic exponents, that vary between 0.4 and 0.6. K_G^e and K_B^e are the shear and bulk modulus numbers, respectively. Unloading in this model is assumed to be purely elastic.

Plastic response

Plastic strains are controlled by the yield loci, which are assumed to be radial lines, starting at the origin of the stress space. For first-time loading, the yield locus is defined by the current stress state of the soil. As the shear stress increases, the stress-ratio (η), given by $\eta = \tau / \sigma'$, increases as well, activating the primary yield surface based upon isotropic hardening. Consequently, the yield surface is dragged to the new location, expanding the elastic zone of the model. This results in plastic strains, both shear and volumetric. Unloading deactivates the primary yield surface, following an elastic path. A Mohr-Coulomb type failure function is assumed to determine the ultimate strength and state of stress achievable in this model. It is given by,

$$f_f = \sigma'_1 - \sigma'_3 N_{\phi_f} + 2c\sqrt{N_{\phi_f}} \tag{7}$$

where, σ'_1 and σ'_3 are the effective major and minor principal stresses, respectively. The parameter c is the cohesion and N_{ϕ_f} is given by the relation

$$N_{\phi_f} = \frac{1+\sin(\phi_f)}{1-\sin(\phi_f)} \tag{8}$$

where, ϕ_f is the peak friction angle. The flow rule is given by the relation,

$$\frac{d\epsilon_v^p}{d\gamma_s^p} = -\tan(\psi) \tag{9}$$

where, ϵ_v^p and γ_s^p are the plastic volumetric and shear strains, respectively and ψ is the dilatation angle. The phase transformation friction angle, or stress ratio (ϕ_{cv}) and dilatation angle are related by the relation

$$-\sin(\psi) = \sin(\phi_{cv}) - \eta \tag{10}$$

where, η is the developed stress ratio. Additionally, η is bound by the rule $\eta \leq \sin(\phi_f)$.

SHAKE TABLE TEST

The results of the shake table test, performed in a centrifuge at the Rensselaer Polytechnic Institute, are summarised in the work of Gonzales et al. (2002). Tests were commissioned to investigate the behaviour of saturated soils under high confining stresses, simulating deep deposits, in order to alleviate concerns about the liquefaction susceptibility of large embankment dams. The experimental model was approximately 0.33 m in height, simulating a 38 m prototype soil deposit. The prototype consists of uniform, saturated Nevada sand, which was assumed to have a relative density of (D_r) of 55 %. The centrifugal acceleration was 120 g with the column also being subjected to a horizontal acceleration of 24 g in model units, which corresponds to 0.2 g in prototype

units. The frequency of the loading for the prototype was 1.5 Hz for a total of 50 cycles. The experimental results were then compared with a numerical model prediction obtained using the software FLAC and UBCSAND model in the work of Byrne et al. (2004). The current study models the column adopting the material point method. A total of 468 background grid elements were used together with 3429 particles. The base acceleration of the column was applied directly to the particles. The forward-Euler time stepping algorithm was used to integrate the momentum equations with 1% Particle-in-Cell damping (Nairn, 2015) being provided when calculating the particle velocities of both the solid and fluid phases. The numerical results were then compared with the published results (Byrne et al., 2004). The accumulation of excess pore pressure and the reduction of mean effective stresses are observed during the course of the simulation. Isochrones of excess pore pressure build-up and reduction of mean effective stresses are plotted. The schematic of the experimental and numerical setup is shown in Figure 1 that has been utilised in this work. For the numerical work, the height of the column and the values for the input motion are taken with respect to the prototype dimensions.

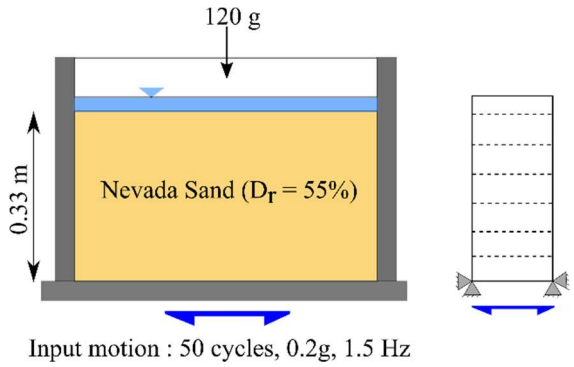

Figure 1 Schematic of experimental and numerical setup of shake table test, performed at the Rensselaer Polytechnic Institute

The isochrones of the mean effective stress at different time intervals obtained from the numerical simulation is presented in Figure 2. Figure 2 presents the reduction of mean effective stress at different time intervals. A reduction in recorded acceleration at different heights of the column that was observed (Byrne et al., 2004; Gonzalez at al., 2002) experimentally was captured in the numerical model. A top-down liquefaction trend, as reported in the experimental works (Gonzales et al., 2002) is captured in the numerical model. Although, numerical instabilities are recorded in the model at the top of the column at the end of the simulation, when the effective stresses are close to being zero, the results obtained in general are in good agreement with what has been observed in the experimental work.

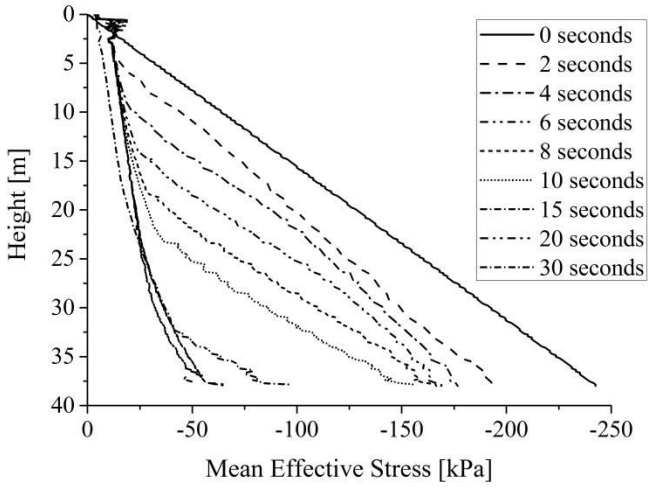

Figure 2 Numerical simulation of shake table test, performed at the Rensselaer Polytechnic Institute: Reduction of mean effective stresses throughout the column at different time intervals

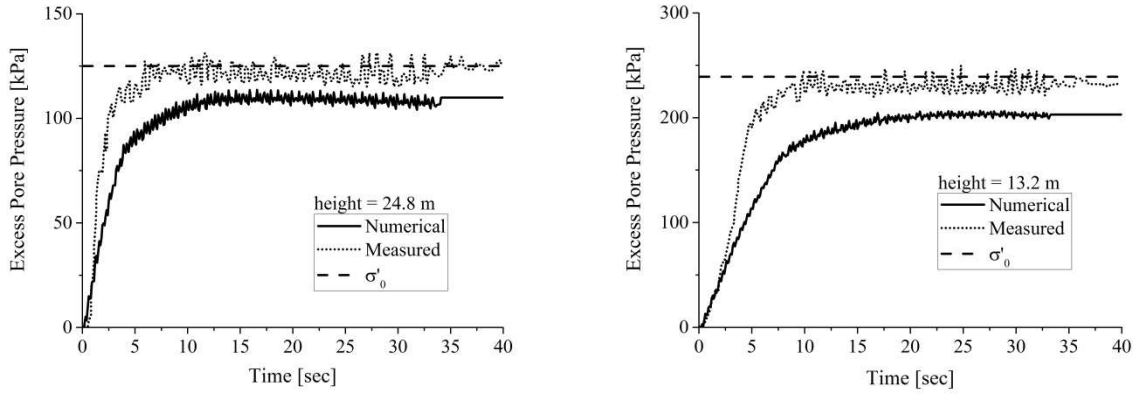

Figure 3 Evolution of Excess Pore Pressure at heights 13.2 m and 24.8 m

Plotting the results of excess pore pressure evolution at two different heights shed light upon the numerical method's capability to reproduce the rate of liquefaction when compared to the experimental results, which are obtained from the work of Byrne et al. (2004). In both the graphs, one can observe that the maximum recorded excess pore pressure from the numerical solution is a bit less than what has been observed in the experimental work. This is consistent with the fact that the effective stresses, as shown in Figure 3, do not drop all the way to zero in these regions. This difference, however, can be corrected by better calibrating the parameters to obtain a closer fit to the experimental values.

Looking at the rate of generation of excess pore pressure from Figure 3, at a height of 13.2 m, the initial rate of generation of excess pore observed in the simulation is close to what has been recorded in the experimental values, but stays constant until the end of the simulation, however the final values of the excess pore pressures between experiment and numerics is different. The rate of liquefaction observed numerically at a height of 24.8 m however, stays constant and is slower than what has been observed in the experiment. In both the graphs however, one can observe that the maximum excess pore pressure attained by the model occurs roughly at the same time when compared to the experimental work. These results indicate that the two-phase CPDI method that has been implemented along with the UBCSAND model that has been adopted is able to capture the liquefaction effects to a reasonable degree of accuracy.

ON USE OF HYPOPLASTIC SOIL MODEL FOR SEISMIC LOADING

While UBCSAND model is capable of capturing the liquefaction effects during dynamic loading, the HPS model enjoys the advantage of being widely available for use in commercial FE software, soil parameters are available for a large number of soil types, calibration routines being available that aid in simplifying the process of parameter calibration, and from a soil mechanics point of view, the HPS models is able to take into account effects like change in void ratio, which the UBCSAND model is not able to capture. The results of undrained triaxial compression and cyclic simple shear test using the HPS model are presented in the work of Tsegaye et al. (2010) where the potential to apply the HPS model for simulations involving liquefaction phenomena was highlighted. Hleibieh et al. (2014) has shown the applicability of the HPS model for the numerical simulation of a tunnel under seismic loading. Nagula et al. (2017) has applied the HPS model assuming saturated sand for liquefaction mitigation study. In this work, the UBCSAND parameters are calibrated to the Berlin sand properties and the numerical results of a shake table test obtained from the UBCSAND model and the HPS model is compared. This would allow us to make a fair comparison for simulation of seismic structures using different constitutive models, and judge the capability of the CPDI method to capture the liquefaction effects using the HPS model. As an additional advantage of the study, the calibration routine of the UBCSAND model can be evaluated by comparing the results from both the constitutive models.

In the work of Winde (2015), the parameters of the HPS model were calibrated to the Fraser river sand to obtain a comparison of the behaviour of the HPS model and UBC3D-PLM model under seismic loading. In this work

however, the UBCSAND model is calibrated to the Berlin sand's properties. A choice here was made to calibrate the UBCSAND to known, high quality data of Berlin sand, instead of calibrating the HPS model to the Nevada sand. The reason for this being one of the goals of this study was to evaluate the implementation of the UBCSAND model used in the framework of multi-phasic CPDI method under seismic loading, and that dwelling upon calibrating another constitutive model would not yield tangible results towards the research goal. Additionally, this study will also serve as a verification step for the calibration routine of the UBCSAND model.

The data for calibration against the Berlin sand were obtained from the work of Le (2015). The monotonic and cyclic tests were chosen for the Berlin sand of relative density I_d = 75%. The parameters for the HPS parameters were obtained from work of Le (2015) as well. The initial calibration procedure for the UBCSAND model were obtained from the work of Shriro et al. (2013) to get the reference values for the stiffness parameters and stress exponents. These values were later refined so that the behaviour of the model was a close fit to the published results. Parameters for the UBCSAND model that was calibrated against Berlin sand used in this simulation are given in Table 1.

Table 1 Parameters for UBCSAND model

$(N1)_{60}$[-]	me [−]	ne [−]	np [−]	K_G^e[−]	K_B^e[−]
11.5	0.5	0.5	0.4	1224	1120
K_G^p[−]	ϕ_{pt}[°]	ϕ_f[°]	c [kPa]	Pa [kPa]	σ_t [kPa]
423	31.5	37.5	0	100	0
$hfac_1$[−]	$hfac_2$[−]	$hfac_3$[−]	$hfac_4$[−]	$hfac_5$[−]	$hfac_6$[−]
0.65	0.85	1.0	0.6	1.0	0.95

The simulation was carried out as elaborated in the previous section. The boundary and the loading conditions for the simulation remain unchanged. For this case, however, the Particle-in-cell damping, which was previously 1%, was doubled and set to 2%. This change was necessitated by reason of the HPS model becoming unstable after a few seconds of simulation. Adding this extra damping immensely aided in improving the stability of the numerical model. The number of particles and the background grid employed remain unchanged from the previous section.

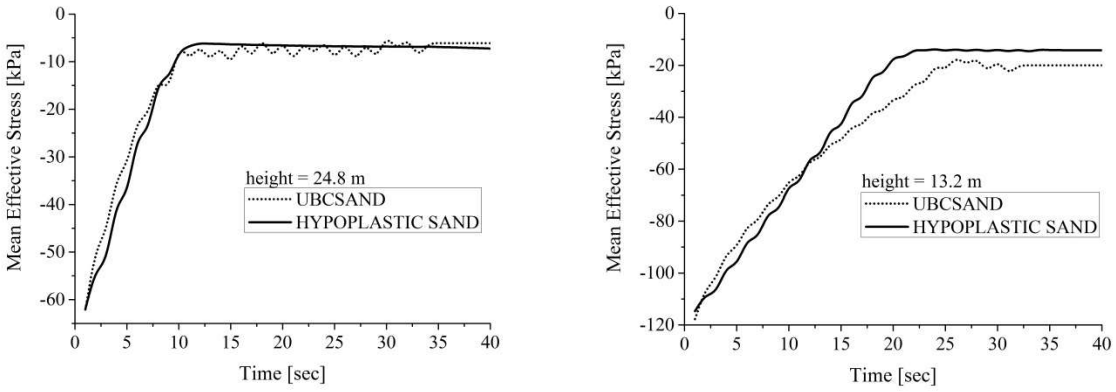

Figure 4 Comparison of the mean effective stress for both models

Figure 4 presents the evolution of mean effective stress for both the HPS model and the UBCSAND model when subjected to dynamic loading. From both graphs, it is clear that the top-down liquefaction approach, is observed here as well with the mean effective stress dropping nearly to zero on the top of the column (24.8 m) before approaching zero on sections below (13.2 m). This behaviour is consistent with the results that have been

experimentally observed for the shake table test shown in Figure 1 It is also clear that the rate at which the soil loses strength on the top section of the column is nearly identical for both the constitutive models, indicating that the calibration of the UBCSAND model has been reasonably accurate for the Berlin sand. The behaviour of the soil at a section that is deeper paints a different picture. The rates at which the UBCSAND and HPS model lose their strength do not seem to agree with each other precisely, and the rate of liquefaction for the HPS model seems to be higher than the UBCSAND model, as shown in Figure 4 at a depth of 13.2 m. The final strength of the soil post-liquefaction also seems to be different from each other, with the HPS model has nearly completely lost its strength, the UBCSAND model hasn't at the same section of the column. This is indicative of incomplete liquefaction. That being said, this phenomenon of residual strength is observed in the previous section, assuming the properties of Nevada sand. It is theorised that a better definition of the material parameters for the UBCSAND that varies with depth, and a better definition of the hardening rule might yield better results.

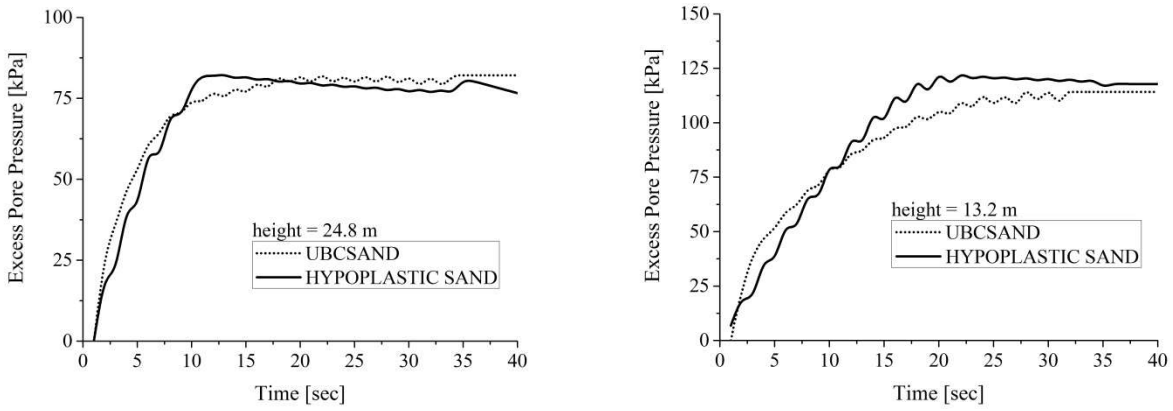

Figure 5 Comparison of excess pore pressure for both models

Figure 5 presents the evolution of the excess pore pressure in both the models. Here again, it is observed that in the top portion of the column (24.8m), the rate of evolution of excess pore pressure for both the models are comparable. Although, one could discern that the rate of evolution of excess pore pressure in the case of HPS model is slightly higher than that of the UBCSAND model. The behaviour of the bottom portion of the section is similar to what has been observed in the evolution of mean effective stresses. The rate of evolution of the excess pore pressure in the case of HPS is slightly higher than the UBCSAND model. This is again consistent with the higher rate of mean effective stress loss in the HPS model. It is concluded that the calibration routine adopted for the UBCSAND is reasonably accurate and that the multi-phasic CPDI code is able to reproduce the liquefaction effects during dynamic loading.

CONCLUSIONS

The UBCSAND model, as published by Naesgaard (2011) was implemented in the CPDI code that included the effects of solid and fluid phases, in a single particle using the *v-w* formulation. The benchmark tests were performed using the multi-phasic CPDI and UBCSAND model and the results were compared against published experimental results. The behaviour of the evolution of excess pore pressure was close to what has been observed in the experiments. Further, the properties for the UBCSAND were calibrated against published data for the Berlin sand. The benchmark test was simulated using the HPS model and the UBCSAND model. The results when compared against each other show a partial agreement with each other, wherein the behaviour was comparable on the top portion of the column, whereas the results were disparate on the bottom portions. It is expected that a better match with the behaviour could be obtained using a better definition of the hardening rule and a depth based material parameter refinement for the UBCSAND model. Future work will involve applying the fully saturated CPDI code towards advanced continuum problems such as the simulation of saturated structures under seismic loading, as well as investigating phenomena like liquefaction in the soil during processes of pile installation.

REFERENCES

Byrne, P.M., Park, S.S., Beaty, M., Sharp, M., Gonzalez, L. and Abdoun, T., 2004. Numerical modeling of liquefaction and comparison with centrifuge tests. *Canadian Geotechnical Journal*, *41*(2), pp.193-211.
Gonzalez, L., Abdoun, T. and Sharp, M.K., 2002. Modelling of seismically induced liquefaction under high confining stress. *International Journal of Physical Modelling in Geotechnics*, *2*(3), pp.01-15.
Hleibieh, J., Wegener, D. and Herle, I., 2014. Numerical simulation of a tunnel surrounded by sand under earthquake using a hypoplastic model. *Acta Geotechnica*, *9*(4), pp.631-640.
Le, V.H., 2015. Zum Verhalten von Sand unter zyklischer Beanspruchung mit Polarisationswechsel im Einfachscherversuch. PhD Thesis, Institut für Bauingenieurwesen, TU Berlin, Germany.
Moormann, C., Gowda, S. and Giridharan, S. (2018). Numerical simulation of pile installation in saturared soil using CPDI. In *Numerical Methods in Geotechnical Engineering IX, Proceedings of the 9th European Conference on Numerical Methods in Geotechnical Engineering (NUMGE), Porto, Portugal 25-27 June 2018, London : Taylor & Francis Group, 2018, pp. 665-672*.
Naesgaard, E., 2011. *A hybrid effective stress–total stress procedure for analyzing soil embankments subjected to potential liquefaction and flow*. PhD Thesis, Department of Civil Engineering, University of British Columbia, Canada.
Nairn, J.A., 2015. Numerical simulation of orthogonal cutting using the material point method. *Engineering Fracture Mechanics*, *149*, pp.262-275.
Nagula, S. and Grabe, J., 2017. 2-Phase dynamic simulation of deep sand compaction to reduce liquefaction. *Procedia Engineering*, *199*, pp.2396-2401.
Puebla, H., Byrne, P.M. and Phillips, R., 1997. Analysis of CANLEX liquefaction embankments: prototype and centrifuge models. *Canadian Geotechnical Journal*, *34*(5), pp.641-657.
Sadeghirad, A., Brannon, R.M. and Burghardt, J., 2011. A convected particle domain interpolation technique to extend applicability of the material point method for problems involving massive deformations. *International Journal for Numerical Methods in Engineering*, *86*(12), pp.1435-1456.
Shriro, M. and Bray, J.D., 2013. Calibration of Numerical Model for Liquefaction-Induced Effects on Levees and Embankments.
Tsegaye, A.B., Molenkamp, F., Brinkgreve, R.B.J., Bonnier, P.G., de Jager, R. and Galavi, V., 2010. Modeling liquefaction behaviour of sands by means of hypoplastic model. *7th European Confrerence on Numerical Methods in Geotechnical Engineering, Trondheim, Norway*, pp.81-87.
van Esch, J., Stolle, D. and Jassim, I., 2011. Finite element method for coupled dynamic flow-deformation simulation. In *2nd International Symposium on Computational Geomechanics (COMGEO II)* (No. 1).
Winde, H.P., 2015. Finite element modelling for earthquake loads on dykes. Master's Thesis, Department of Hydraulic Engineering, TU Delft, The Netherlands.
Zienkiewicz, O.C., Chan, A.H.C., Pastor, M., Paul, D.K. and Shiomi, T., 1990. Static and dynamic behaviour of soils: a rational approach to quantitative solutions. I. Fully saturated problems. *Proc. R. Soc. Lond. A*, *429*(1877), pp.285-309.